Memory signals are temporally dissociated in and across human hippocampus and perirhinal cortex

Bernhard P Staresina[1,2], Juergen Fell[2], Anne T A Do Lam[2], Nikolai Axmacher[2,3] & Richard N Henson[1]

In the endeavor to understand how our brains enable our multifaceted memories, much controversy surrounds the contributions of the hippocampus and perirhinal cortex (PrC). We recorded functional magnetic resonance imaging (fMRI) in healthy controls and intracranial electroencephalography (EEG) in patients during a recognition memory task. Although conventional fMRI analysis showed indistinguishable roles of the hippocampus and PrC in familiarity-based item recognition and recollection-based source retrieval, event-related fMRI and EEG time courses revealed a clear temporal dissociation of memory signals in and across these regions. An early source retrieval effect was followed by a late, post-decision item novelty effect in hippocampus, whereas an early item novelty effect was followed by a sustained source retrieval effect in PrC. Although factors such as memory strength were not experimentally controlled, the temporal pattern across regions suggests that a rapid item recognition signal in PrC triggers a source retrieval process in the hippocampus, which in turn recruits PrC representations and/or mechanisms, evidenced here by increased hippocampal-PrC coupling during source recognition.

Our memories range from a vague feeling of familiarity for a face in a crowd to recollecting specific details of a previous encounter. Although the critical role of the medial temporal lobes (MTL) for these different expressions of memory is well established[1,2], much controversy surrounds the precise contributions of different MTL subregions, most notably the hippocampus and the adjacent PrC. Considerable evidence points to a role of the hippocampus in associative memory processes[3,4], which are also referred to as source memory[5], relational memory[6] or recollection-based memory[7,8]. The common tenet of these theories is that the hippocampus is needed for the retrieval of multiple event details, but not for simple old versus new identification of individual items (also referred to as item- or familiarity-based recognition). However, recent neuropsychological and fMRI studies have challenged the notion that the hippocampus has an exclusive role in source memory, demonstrating that patients with selective hippocampal damage can also show impaired item memory[9,10] and that hippocampal fMRI responses can be explained by memory strength alone[11,12]. One way to resolve this issue is to investigate the temporal profiles of item effects in the hippocampus. In particular, theoretical accounts[13–15], behavioral data[15,16] and electrophysiological scalp recordings[17] suggest that a familiarity-based item signal occurs rapidly, whereas recollection-based source memory occurs later, requiring more sustained engagement.

A similar controversy surrounds the role of the PrC in memory. Some theories suggest that this region is dedicated specifically to familiarity-based item recognition (just as the hippocampus is dedicated specifically to recollection-based source memory)[7,8,18], whereas others suggest that PrC can support both item and source memory, as long as the critical information is object related[3,19,20].

One approach to reconcile these views has been to postulate that perirhinal involvement in source memory tasks actually reflects enhanced familiarity for object-related associations[21]. If so, perirhinal source effects should occur at the same latency as simple old/new effects (both reflecting familiarity).

We assessed the roles of the hippocampus and PrC by examining the temporal profiles of item and source memory signals in these regions during recognition memory. To this end, we employed the same memory task to probe both item recognition and source memory during fMRI recordings in healthy participants and during intracranial EEG (iEEG) recordings obtained directly from the hippocampus and PrC of presurgical epilepsy patients (**Fig. 1**). Both methods converged on the same temporal pattern of item and source effects in and across these regions, supporting a role of the hippocampus specifically in recollection-based source retrieval, and a role of the PrC not only in rapid familiarity-based item recognition, but also in later recollection-based source retrieval.

RESULTS

Our attempts to match memory performance across iEEG (patient) and fMRI (control) groups (by varying the number of sources, retention interval and encoding list length; see Online Methods) were successful (**Table 1**). A probability measure (probability of correct minus probability of incorrect old decisions to studied items) revealed that overall recognition memory was significantly above chance (0) (fMRI, $70 \pm 4\%$, $t_{19} = 16.18$, $P < 0.001$; iEEG, $62 \pm 9\%$, $t_4 = 6.56$, $P = 0.003$). Probability for source recognition (probability of correct minus incorrect source decisions to studied items excluding "don't know" responses) was also significantly above chance (fMRI, $74 \pm 6\%$, $t_{19} = 13.46$, $P < 0.001$; iEEG, $52 \pm 8\%$, $t_4 = 6.15$, $P = 0.004$).

Figure 1 Methods and design. (**a**) fMRI ROIs (highlighted in yellow) for hippocampus and PrC of an example participant. (**b**) iEEG electrode locations. Left, medial temporal lobe implantation scheme used for all participants. Middle, hippocampus and PrC contacts of an example participant, shown on the post-implantation MRI scan. Right, same contacts shown on the co-registered pre-implantation MRI scan. Anatomical images in **a** and **b** are normalized for comparability. (**c**) Experimental design (iEEG version). During the study phase, participants saw concrete nouns together with an associated source (a color in half of the runs and a scene in the other half of the runs) and indicated whether or not the combination was plausible. During the test phase, from which the present data were analyzed, studied (old)

words were shown along with unstudied (new) words, and participants indicated, with one button press, whether they remembered the word from the study phase and whether they remembered its associated source. Conditions of interest were correct rejection of new items (correct rejection), correct identification of old items without remembering the associated source (item recognition) and correct identification of old items plus remembering the associated source (source recognition). Note that procedural details differed slightly between fMRI and iEEG versions of the experiment (see Online Methods) to allow for the different signal characteristics and to match behavioral performance across controls and patients.
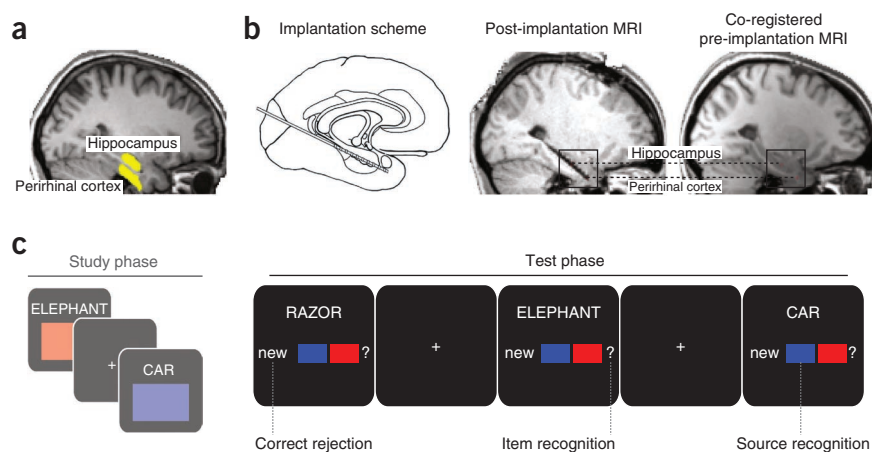
No significant differences were observed in item or source probability measures across fMRI and iEEG groups (both $t_{23} < 1.63$, $P > 0.11$). For further analyses, trials in which an item was recognized (hit), but either a "don't know" response or an incorrect source response was given, were collapsed, and are referred to as item recognition.

For all imaging analyses, we defined two memory effects of interest: an item effect (that is, the difference between correct rejection and item recognition, which emphasizes processes related to simple item recognition or novelty detection while reducing the effect of target source retrieval) and a source effect (that is, the difference between source recognition and item recognition, which emphasizes processes related to retrieval of target source details while reducing the effect of item recognition and novelty).

For our fMRI data, we first queried item and source memory effects via a conventional analysis of the blood oxygenation level–dependent (BOLD) response based on an assumed hemodynamic response function (HRF). We extracted the mean parameter estimates across voxels in each region of interest (ROI), where ROIs were defined anatomically and separately for each participant, based on their structural MRI (**Fig. 2**). No hemispheric differences were seen in this or any subsequent analysis (**Supplementary Results**), so we averaged data across left and right ROIs. We found that both hippocampus and PrC exhibited a significant item effect (both $t_{19} > 2.41$, $P < 0.05$) as well as a significant source effect (both $t_{19} > 2.18$, $P < 0.05$), resulting in a U-shaped pattern across correct rejection–item recognition–source recognition.

We then assessed whether item and source effects might show different temporal BOLD profiles. As would be expected from the above results, the integrated BOLD signal (averaged from 3–9 s post stimulus onset) in both hippocampus and PrC revealed a significant item effect

(both $t_{19} > 2.91$, $P < 0.01$) and a significant source effect (both $t_{19} > 3.27$, $P < 0.005$). More critically, however, our data revealed that these effects have different temporal characteristics within and across regions (**Fig. 2**). In the hippocampus, the item effect was delayed relative to the source effect, whereas there was an early and transient item effect in the PrC, together with a more sustained source effect. These temporal dissociations within regions were confirmed by a repeated-measures ANOVA with the factors effect (item, source) and time (repetition time 1–4), which revealed significant effect × time interactions in both regions (both $F_{3,57} > 4.61$, $P < 0.01$). Moreover, the BOLD data showed that the sequence of item and source effects differs across the two regions, as evidenced by a significant region × effect × time interaction ($F_{3,57} = 3.83$, $P = 0.01$). Comparing the latencies of each participant's effect peak (using a nonparametric Wilcoxon test), we observed that the PrC item effect peaked significantly earlier than the hippocampal source effect ($P = 0.02$), whereas the PrC source effect peaked significantly earlier than the hippocampal item effect ($P < 0.005$). Nonetheless, inferring the latency of neural activity from the temporal characteristics of the BOLD response is difficult (given potential nonlinear neural-vascular mappings[22]). Thus, to better explore the temporal profiles of memory signals in the hippocampus and PrC, we capitalized on the real-time resolution of the iEEG data.

We first defined two time windows of interest: an early window ranging from 250–750 ms post stimulus onset that encompassed the initial peak responses in both hippocampus and PrC when collapsing across conditions (**Supplementary Fig. 1a**), and a late window ranging from 800–2,000 ms post stimulus onset that captured a sustained, second component in both regions (**Supplementary Fig. 1b**). As in the fMRI data, no hemispheric differences were seen (**Supplementary Results**).

Table 1 Behavioral results for fMRI and iEEG version of the experiment

| | Studied items | | Unstudied items | | Source memory out of hits | | | Reaction times (s) | | |
| | | | | | | IR | SR | | | |
	Hit	Miss	CR	False alarm	"?" response	Source incorrect	Source correct	CR	IR	SR
fMRI	87 (3)	13 (3)	82 (3)	18 (3)	35 (3)	9 (2)	56 (4)	1.72 (0.08)	2.27 (0.06)	1.90 (0.07)
iEEG	82 (6)	18 (6)	80 (10)	20 (10)	42 (11)	14 (4)	43 (8)	1.65 (0.19)	2.10 (0.17)	1.86 (0.20)

Memory performance is expressed in percentage of old or of new items. Standard errors are shown in parentheses. CR, correct rejection; IR, item recognition; SR, source recognition.
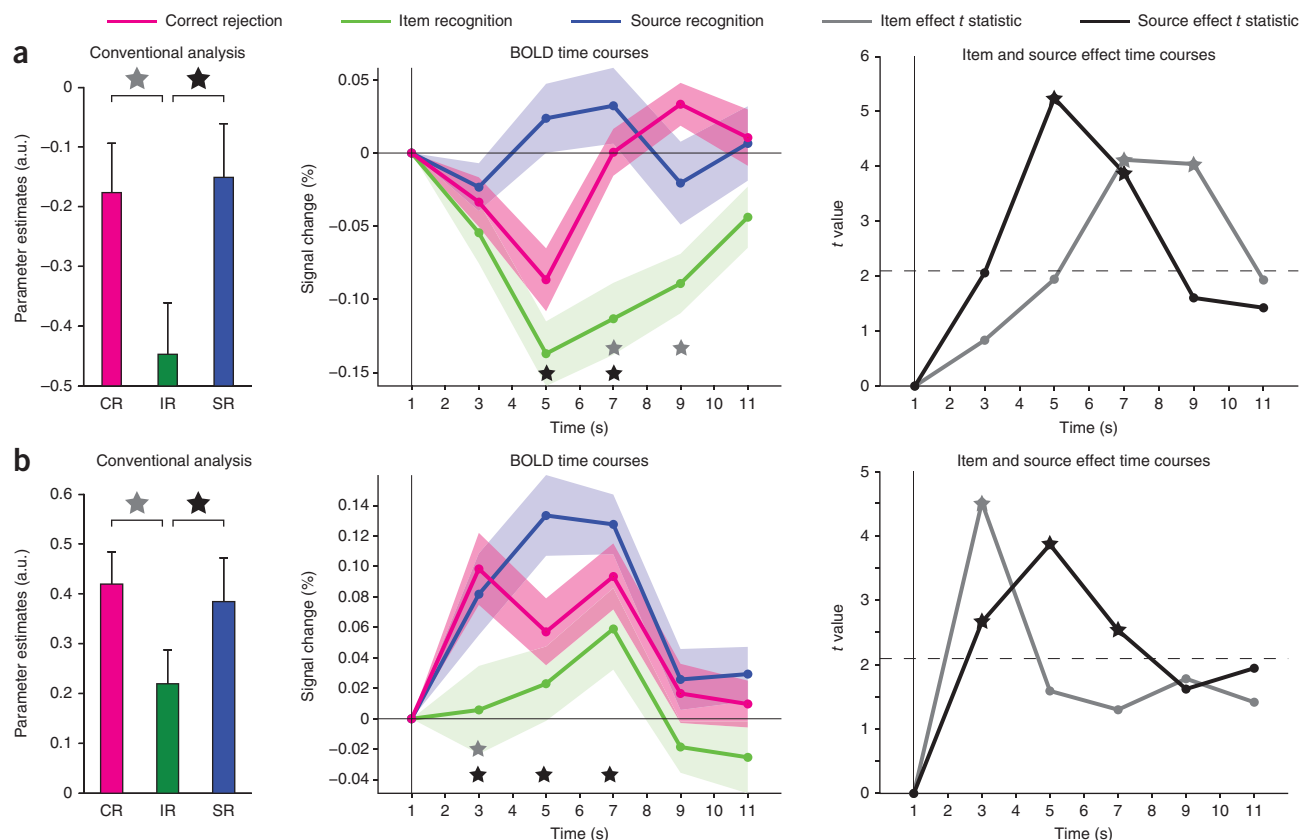
Figure 2 fMRI results for hippocampus and PrC. (**a,b**) Left, results from modeling conditions in a conventional analysis using an assumed HRF for hippocampus (**a**) and PrC (**b**). Bar graphs represent mean + s.e.m. parameter estimates. Note that, although differing with respect to baseline, item effects (correct rejection versus item recognition) and source effects (source recognition versus item recognition) were indistinguishable in or across regions. Middle, average ± s.e.m. fMRI BOLD time courses versus baseline for the three conditions of interest. Right, statistical development of the item effect (differential evoked response for correct rejection versus item recognition) and source effect (source recognition versus item recognition), showing *t* values for each effect across time. Points above the dashed line correspond to *P* < 0.05, two tailed. Gray stars indicate a significant item effect (correct rejection versus item recognition) and black stars indicate a significant source effect (source recognition versus item recognition, *P* < 0.05). Note the temporal dissociation of item and source effects in and across regions. a.u., arbitrary units.

In the hippocampus (**Fig. 3a**), the early analysis window (250–750 ms) showed a significant source effect (t_4 = 4.88, P = 0.008), but we found no evidence of an item effect (t_4 = 0.05, P = 0.960). In the late analysis window (800–2,000 ms), the item effect was significant (t_4 = 3.17, P = 0.034), whereas the source effect no longer reached significance (t_4 = 1.82, P = 0.142). The late onset of the item effect suggests that this hippocampal response might reflect post-retrieval processes for new items, rather than the fast identification of old items that is expected by the behavioral evidence for rapid familiarity-based recognition. To assess more directly whether the hippocampal item effect reflects post-retrieval processes, we compared item and source effects in response-locked (instead of stimulus-locked) event-related potentials (ERPs). More specifically, we compared a 500-ms time window from −750 ms to −250 ms with that from +250 ms to +750 ms, defined relative to the participants' key press on each trial. We observed an inter-action between time window (pre, post) and effect (item, source) ($F_{1,4}$ = 11.07, P = 0.029), as the pre-response window showed a source effect (t_4 = 3.49, P = 0.025), but no item effect (t_4 = 1.09, P = 0.339), and the post-response window showed an item effect (t$_4$ = 3.33, P = 0.029), but no source effect (t_4 = 0.95, P = 0.398). This result suggests that the hippocampal source effect precedes the memory judgment, whereas the item effect only occurs after the memory

judgment, and therefore likely reflects processes such as incidental encoding of experimentally novel information (see Discussion).

In the PrC (**Fig. 3b**), the early time window (250–750 ms) showed both an item effect (t_4 = 5.82, P = 0.004) and a source effect (t_4 = 3.20, P = 0.033). In the late time window (800–2,000 ms), the source effect was still significant (t_4 = 5.30, P = 0.006), whereas the item effect was not (t_4 = 0.34, P = 0.752). For the response-locked analysis, there was, unlike in the hippocampus, no differential size of source versus item effects with respect to pre- versus post-response time windows ($F_{1,4}$ = 0.12, P = 0.743); only a main effect of time window ($F_{1,4}$ = 12.12, P = 0.025), reflecting the fact that the com-bined item and source effects were stronger in the pre- than in the post-response time window. However, only the source effect reached significance in the pre-response time window (t_4 = 7.46, P = 0.002), whereas the item effect did not (t_4 = 2.24, P = 0.088), suggesting that the source effect was sustained and terminated with the memory response compared with a rapid and transient item effect.

To further investigate the latency of these effects, we calculated the earliest time point that showed a reliable item and source effect in each region. The first effect was an item effect in PrC at 200 ms post stimulus onset. Next, we observed a source effect in the hippocampus at 250 ms, followed by a source effect in PrC at 400 ms. A hippocampal item effect was first observed at 1,050 ms (**Fig. 4**).

Figure 3 iEEG results for hippocampus and PrC. (**a,b**) Left, stimulus-locked ERPs for hippocampus (**a**) and PrC (**b**). Right, response-locked ERPs. Shaded areas show the two time windows used for statistical analysis. Data are presented as in **Figure 2**.

In summary, although item and source effects were indistinguishable within and across regions via conventional fMRI analysis, time-resolved BOLD data showed that these effects can be temporally dissociated. This dissociation was confirmed by our iEEG findings. In the hippocampus, we observed an early source effect that terminated with the participants' memory response and an item effect that onset much later in the trial, after the memory decision had been made. In PrC, our data suggest that there might be two independent processes: a fast and transient item effect and a later-onset source effect that is sustained throughout the retrieval period and terminates with participants' memory decision. Thus, although both regions seem to conjointly support source retrieval (see below), the item effect appears to reflect different processes in each case: a fast novelty signal in PrC and a late, post-retrieval encoding process in the hippocampus.

To test the notion that successful source retrieval is accompanied by increased functional coupling across hippocampus and PrC, we conducted connectivity analyses using both fMRI and iEEG data. For the fMRI data, we used a psychophysiological interaction (PPI) analysis (see Online Methods). Using the individually and anatomically defined hippocampi as seed regions, we identified a set of bilateral PrC clusters with greater functional coupling with the hippocampus during source recognition versus item recognition ($P_{corrected} = 0.042$;
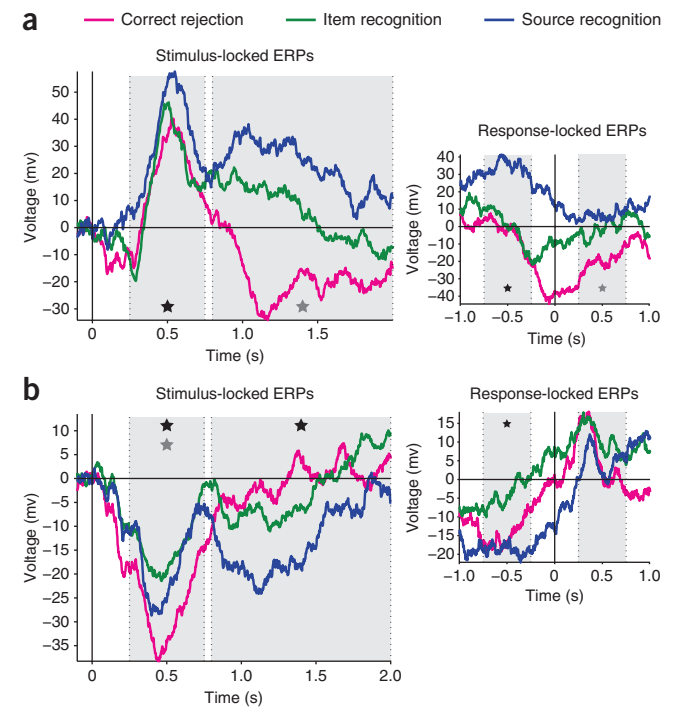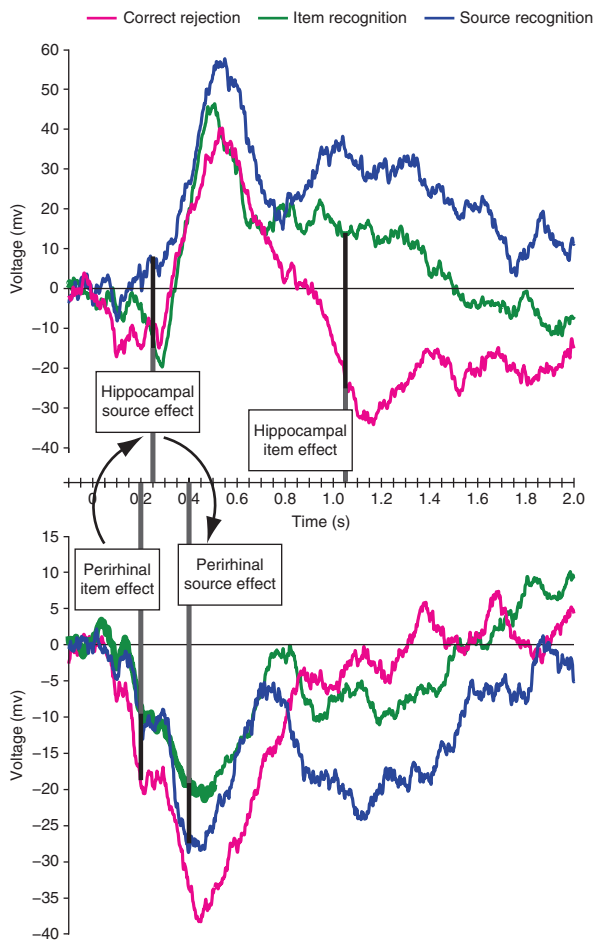
Fig. 5a). No differences in hippocampal-perirhinal coupling were observed for the item effect (correct rejection versus item recognition) at $P < 0.001$, uncorrected.

We conducted spectral coherence analysis using our iEEG data (see Online Methods). For the comparison of source recognition versus item recognition, this analysis revealed two clusters ($P < 0.05$, corrected via a cluster-based statistic across time and frequencies[23]; see Online Methods) in which coherence differed significantly across conditions (**Fig. 5b,c**). First, source recognition showed greater coherence between hippocampus and PrC in the low gamma band (30–35 Hz) from ~700 to 800 ms. Second, we observed increased coherence for item recognition, or, conversely, increased decoupling for source recognition, between hippocampus and PrC in the alpha band (8–12 Hz) from ~500 to 900 ms. Because the temporal resolution of spectral analysis is inferior to that of ERPs, we refrain from making strong conclusions about the timing of these gamma- and alpha-coupling effects, but it is worth noting that both effects overlapped in time and coincided with the period in which both regions showed differential ERPs for source recognition versus item recognition. The increase in low gamma coupling for successful source recognition is consistent with previous findings during successful relative to unsuccessful memory encoding[24,25], and the inverse alpha coupling effect (greater for unsuccessful source recognition) is interesting in light of the emerging role of alpha oscillations in functional inhibition of brain regions[26]. Again, no changes in coherence were observed for correct rejection versus item recognition (using the same statistical threshold as for source recognition versus item recognition). Together, our fMRI and iEEG connectivity results provide strong support for the notion that successful source retrieval is accompanied by an increase in functional coupling between hippocampus and PrC.

Figure 4 Temporal sequence of iEEG item and source effects in PrC and hippocampus. Top, hippocampus; bottom, PrC. ERPs are identical to those shown in **Figure 3** (left). Vertical lines demarcate the onset of the first statistically reliable item and source effect in each region. The darker portions of vertical lines highlight the relevant condition differences.

Figure 5 Functional coupling between hippocampus and PrC increases during source recognition (source recognition versus item recognition). (**a**) MTL regions showing a PPI using participants' individually drawn hippocampi as seed regions (schematized in the sagittal view, right). Results are shown at $P < 0.001$ (uncorrected) for display purposes. Left peak: $x = -27$, $y = 2$, $z = -35$; right peak: $x = 21$, $y = 2$, $z = -38$. (**b**) Time by frequency clusters of significant iEEG coherence differences between source recognition versus item recognition ($P < 0.05$, corrected for multiple comparisons). Color reflects absolute t values for source recognition versus item recognition (only significant t values are shown). (**c**) Average ± s.e.m. time course of coherence in the significant clusters. Left, coherence in the low gamma band (30–35 Hz) was enhanced for source recognition relative to item recognition between ~700 and 800 ms. Right, coherence in the alpha band (8–12 Hz) was reduced for source recognition relative to item recognition between ~500 and 900 ms.
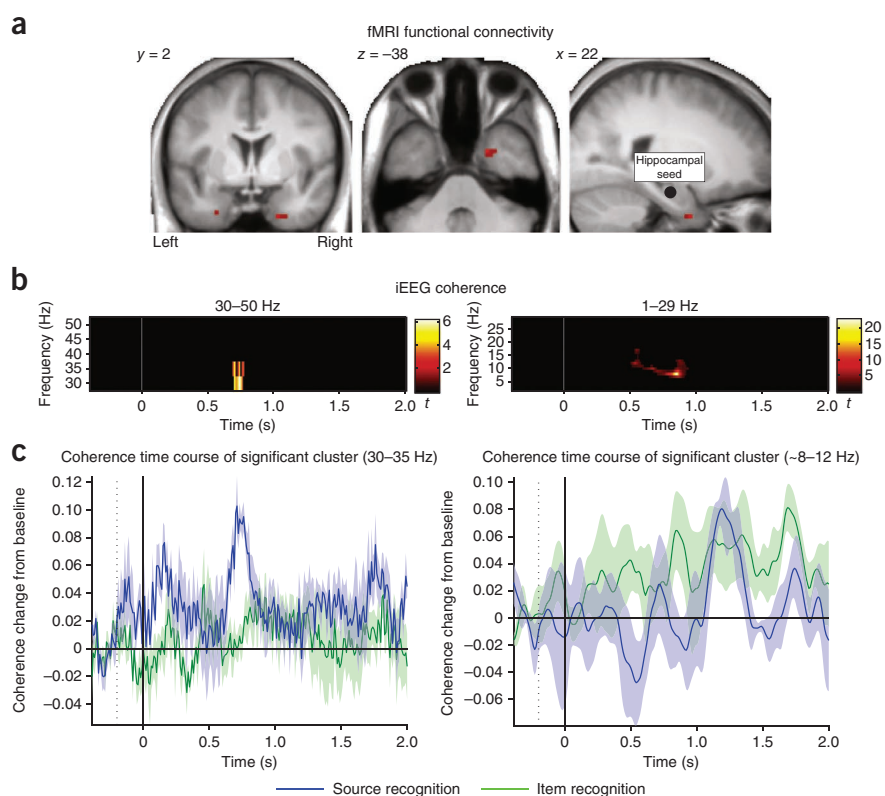
DISCUSSION

Using the same memory task during fMRI recordings in healthy participants and iEEG in patients (**Fig. 1**), we sought to elucidate the functional contributions of the hippocampus and PrC to recognition memory. Consistent with previous fMRI studies[11,27], item and source memory signals were indistinguishable within and across regions when applying a conventional fMRI analysis (**Fig. 2**). However, a more fine-grained latency analysis revealed a temporal dissociation of item and source memory effects within and across hippocampus and PrC, both in BOLD time course data (**Fig. 2**) and, with much superior temporal resolution, in iEEG recordings (**Fig. 3**). The latency of the perirhinal item effect was short enough to provide, consistent with behavioral[16] and neural[17,28] evidence, a rapid familiarity/novelty signal. The hippocampal item effect, on the other hand, emerged too late to be likely to contribute to the recognition decision—indeed, it was only reliable after rather than before that decision—and thus more likely reflects post-retrieval encoding of new items[29,30].

We operationalized the item effect as the difference between correct rejection of experimentally novel items (correct rejection) and item recognition without remembering the associated source (item recognition). Nonetheless, it is conceivable that item recognition trials were also accompanied by retrieval of nontarget source details or by increased source retrieval effort[4]. Similarly, although our source effect was operationalized as the difference between item recognition and item recognition along with successful source memory (source recognition), it is conceivable that source recognition trials also exceed item recognition in terms of overall memory strength[11]. Although we did not obtain continuous measures of source memory or memory strength, and so cannot rule out the contribution of either to our results, we note that neither is sufficient as the sole explanation of the complete pattern of condition effects across perirhinal and hippocampal regions. In other words, although any contrast of experimental conditions is unlikely to be process pure, our pattern of data is inconsistent with a single, common factor (such as memory strength) driving activity in both hippocampus and PrC.

The hippocampus showed an early (onset at 250 ms) source effect (increase for source recognition relative to item recognition), which is consistent with this region's established role in associative-, contextual- and recollection-based memory[3,6–8,18,31]. Notably, the hippocampus also showed a strong response to novel items (correct rejection versus item recognition), but this effect did not emerge until 1,050 ms post stimulus onset. This late negative component (LNC) for new items relative to old items has been observed in iEEG recordings[32], but has never been related to item versus source memory. Given the inverted polarity of the iEEG item effect relative to the earlier source effect, one possibility is that the LNC might be mediated by a different cell population in the hippocampus. Indeed, single-unit recordings from human hippocampus during recognition memory procedures have identified two cell types: one type producing greater firing rates for old items (old selective) and the other type producing greater firing rates for new items (new selective)[33,34]. Notably, our findings extend these single-unit data in two ways. First, regarding the new-selective response, this signal seems unlikely to support novelty detection *per se*, considering the latency of the LNC (~800 ms after the source effect). That is, the new-selective response is unlikely to be a purely stimulus-driven response. Rather, the hippocampal response to (correctly rejected) unstudied items seems likely to support incidental, episodic encoding processes (that occur even during a recognition memory test[29,30]), which is corroborated by our finding that this item effect/novelty response unfolds after the memory decision has been made (**Fig. 3a**). Note that, although these results argue against a role of the hippocampus in rapid, familiarity-based item recognition, they are not incompatible with the established role of the hippocampus in detection of other types of (contextual) novelty, such as context deviancy[35], configural novelty[36] or prediction error[37]. Second, regarding the hippocampal old-selective response, our data suggest that this response may largely reflect source retrieval rather than simple item recognition. That is, although the hippocampal peak response

would resemble a basic item-recognition response when collapsing item recognition and source recognition into a single 'old' bin (as in previous iEEG studies[32,38]), separation of item recognition and source recognition suggests that this response is in fact driven by events in which successful associative/source retrieval occurs.

Prevalent models of the PrC postulate a role for this region in familiarity-based recognition[7,8] or in coding for weak rather than for strong memories[11]. To the extent that both familiarity and memory strength increase from correct rejection of an unstudied item (correct rejection) to item recognition and from item recognition to source recognition, the early effect pattern we observed in our iEEG data (item recognition < source recognition < correct rejection) is partially incompatible with both views. An alternative scenario, however, is that PrC independently supports both item recognition via decreased neural activity for studied (experimentally familiar) relative to unstudied (experimentally novel) stimuli (item recognition < correct rejection) and source memory via enhanced activity for successful relative to unsuccessful retrieval of associated event details (source recognition > item recognition). The first role (item recognition through decreased activity, or conversely, increased activity for experimentally novel stimuli) has received considerable support from a variety of methods. For instance, neurons in the primate PrC have been shown to decrease their firing rates as a function of stimulus repetition[28], and lesions to the primate PrC result in marked object recognition deficits[39,40]. Moreover, human fMRI studies have reported reduced BOLD signals for old relative to new items[41–43], while previous iEEG studies in human epilepsy patients have reported reduced N400 components for old relative to new items[32,44]. Thus, our finding of a reduced perirhinal response for item recognition relative to correct rejection is compatible with this region's established role in (familiarity based) item recognition. However, a more recent series of findings have suggested a role for PrC in memory processes beyond simple item recognition. For example, single neurons in primate PrC have been shown to code for object-object associations (pair-coding neurons)[45,46]. In addition, recent fMRI studies in humans have shown that PrC can support, in conjunction with the hippocampus, successful associative encoding[47] as well as associative retrieval[27,48]. Thus, converging evidence suggests that the role of PrC in episodic memory may encompass both item and source memory. However, if item and source memory are indeed separate functions of PrC, one might expect these functions to be mediated by separate cell populations and/or to show different temporal and dynamic profiles. Indeed, we found that the item recognition effect (item recognition versus correct rejection) lasted from 200 ms until ~800 ms post stimulus onset, whereas the associative recognition effect (source recognition versus item recognition) started at 400 ms (**Figs. 3b** and **4**) and was sustained throughout the remainder of the trial period, terminating with the memory response. Thus, not only do our data suggest both item and source effects in PrC, but they indicate that item recognition and source retrieval may be partially separable processes supported by this region (possibly in conjunction with the hippocampus).

How do hippocampus and PrC interact during recognition memory? We found that the item effect in PrC preceded the onset of the source effect in the hippocampus, which in turn preceded the onset of the source effect in PrC (**Fig. 4**). This temporal pattern is suggestive of a signaling loop between PrC and hippocampus, in which a rapid item recognition signal in PrC triggers source retrieval processes in the hippocampus, which in turn entrain the PrC in the service of retrieving and/or maintaining an associated source detail. A recent study obtaining intralaminar recordings from primate PrC during a paired associate task found a reversal of the signal flow from a forward signal during the cue period (item processing) to a backward signal during the delay period (when retrieving the paired associate)[49]. Although that study did not record from the hippocampus, our data suggest that this reversal might be triggered by the hippocampus. Indeed, a critical role of the hippocampus in initiating source retrieval is consistent with single-unit data showing that successful free recall is preceded by a gradual increase of hippocampal firing rates[50]. This idea that hippocampus and PrC need to interact during successful source retrieval is further substantiated by our finding of enhanced functional coupling among these regions during source recognition relative to item recognition (**Fig. 5**).

Together, the temporal sequence of an early perirhinal item effect (for example, familiarity signal) followed by a hippocampal source effect (for example, recollection signal) lends strong support to current models that emphasize a functional separation between hippocampus and PrC during episodic memory processes[3,4,7,8,18]. However, the subsequent source effect in PrC, along with increases in functional coupling between hippocampus and PrC, also highlight the intricate interaction of these regions that underlies the retrieval of episodically rich memory traces.

METHODS

Methods and any associated references are available in the online version of the paper.

Note: Supplementary information is available in the online version of the paper.

AUTHOR CONTRIBUTIONS
B.P.S. and R.N.H. designed the research. B.P.S., N.A., J.F. and R.N.H. wrote the manuscript. B.P.S. conducted the experiments and analyzed the data. A.T.A.D.L. assisted in conducting the iEEG experiments.

1. Scoville, W.B. & Milner, B. Loss of recent memory after bilateral hippocampal lesions. *J. Neurol. Neurosurg. Psychiatry* **20**, 11–21 (1957).
2. Squire, L.R., Stark, C.E. & Clark, R.E. The medial temporal lobe. *Annu. Rev. Neurosci.* **27**, 279–306 (2004).
3. Davachi, L. Item, context and relational episodic encoding in humans. *Curr. Opin. Neurobiol.* **16**, 693–700 (2006).
4. Mayes, A., Montaldi, D. & Migo, E. Associative memory and the medial temporal lobes. *Trends Cogn. Sci.* **11**, 126–135 (2007).
5. Johnson, M.K., Hashtroudi, S. & Lindsay, D.S. Source monitoring. *Psychol. Bull.* **114**, 3–28 (1993).
6. Cohen, N.J. & Eichenbaum, H.E. *Memory, Amnesia and the Hippocampal System* (MIT Press, Cambridge, Massachusetts, 1993).
7. Diana, R.A., Yonelinas, A.P. & Ranganath, C. Imaging recollection and familiarity in the medial temporal lobe: a three-component model. *Trends Cogn. Sci.* **11**, 379–386 (2007).
8. Eichenbaum, H., Yonelinas, A.P. & Ranganath, C. The medial temporal lobe and recognition memory. *Annu. Rev. Neurosci.* **30**, 123–152 (2007).
9. Manns, J.R., Hopkins, R.O., Reed, J.M., Kitchener, E.G. & Squire, L.R. Recognition memory and the human hippocampus. *Neuron* **37**, 171–180 (2003).
10. Stark, C.E., Bayley, P.J. & Squire, L.R. Recognition memory for single items and for associations is similarly impaired following damage to the hippocampal region. *Learning Mem.* **9**, 238–242 (2002).
11. Squire, L.R., Wixted, J.T. & Clark, R.E. Recognition memory and the medial temporal lobe: a new perspective. *Nat. Rev. Neurosci.* **8**, 872–883 (2007).
12. Wais, P.E., Squire, L.R. & Wixted, J.T. In search of recollection and familiarity signals in the hippocampus. *J. Cogn. Neurosci.* **22**, 109–123 (2010).

13. Jacoby, L.L. A process dissociation framework: separating automatic from intentional uses of memory. *J. Mem. Lang.* **30**, 513–541 (1991).
14. Mandler, G. Recognizing: the judgment of previous occurrence. *Psychol. Rev.* **87**, 252–271 (1980).
15. Yonelinas, A.P. The nature of recollection and familiarity: a review of 30 years of research. *J. Mem. Lang.* **46**, 441–517 (2002).
16. McElree, B., Dolan, P.O. & Jacoby, L.L. Isolating the contributions of familiarity and source information to item recognition: A time course analysis. *J. Exp. Psychol. Learn. Mem. Cogn.* **25**, 563–582 (1999).
17. Curran, T. Brain potentials of recollection and familiarity. *Mem. Cognit.* **28**, 923–938 (2000).
18. Aggleton, J.P. & Brown, M.W. Episodic memory, amnesia and the hippocampal-anterior thalamic axis. *Behav. Brain Sci.* **22**, 425–444 (1999).
19. Duarte, A., Henson, R.N. & Graham, K.S. Stimulus content and the neural correlates of source memory. *Brain Res.* **1373**, 110–123 (2011).
20. Staresina, B.P. & Davachi, L. Object unitization and associative memory formation are supported by distinct brain regions. *J. Neurosci.* **30**, 9890–9897 (2010).
21. Diana, R.A., Yonelinas, A.P. & Ranganath, C. The effects of unitization on familiarity-based source memory: testing a behavioral prediction derived from neuroimaging data. *J. Exp. Psychol. Learn. Mem. Cogn.* **34**, 730–740 (2008).
22. Henson, R.N., Shallice, T., Josephs, O. & Dolan, R.J. Functional magnetic resonance imaging of proactive interference during spoken cued recall. *Neuroimage* **17**, 543–558 (2002).
23. Maris, E. & Oostenveld, R. Nonparametric statistical testing of EEG and MEG data. *J. Neurosci. Methods* **164**, 177–190 (2007).
24. Fell, J. *et al.* Human memory formation is accompanied by rhinal-hippocampal coupling and decoupling. *Nat. Neurosci.* **4**, 1259–1264 (2001).
25. Jutras, M.J., Fries, P. & Buffalo, E.A. Gamma-band synchronization in the macaque hippocampus and memory formation. *J. Neurosci.* **29**, 12521–12531 (2009).
26. Haegens, S., Nácher, V., Luna, R., Romo, R. & Jensen, O. α-Oscillations in the monkey sensorimotor network influence discrimination performance by rhythmical inhibition of neuronal spiking. *Proc. Natl. Acad. Sci. USA* **108**, 19377–19382 (2011).
27. Kirwan, C.B. & Stark, C.E. Medial temporal lobe activation during encoding and retrieval of novel face-name pairs. *Hippocampus* **14**, 919–930 (2004).
28. Xiang, J.Z. & Brown, M.W. Differential neuronal encoding of novelty, familiarity and recency in regions of the anterior temporal lobe. *Neuropharmacology* **37**, 657–676 (1998).
29. Buckner, R.L., Wheeler, M.E. & Sheridan, M.A. Encoding processes during retrieval tasks. *J. Cogn. Neurosci.* **13**, 406–415 (2001).
30. Stark, C.E. & Okado, Y. Making memories without trying: medial temporal lobe activity associated with incidental memory formation during recognition. *J. Neurosci.* **23**, 6748–6753 (2003).
31. Konkel, A. & Cohen, N.J. Relational memory and the hippocampus: representations and methods. *Frontiers in Neuroscience* **3**, 166–174 (2009).
32. Ludowig, E. *et al.* Intracranially recorded memory-related potentials reveal higher posterior than anterior hippocampal involvement in verbal encoding and retrieval. *J. Cogn. Neurosci.* **20**, 841–851 (2008).
33. Rutishauser, U., Schuman, E.M. & Mamelak, A.N. Activity of human hippocampal and amygdala neurons during retrieval of declarative memories. *Proc. Natl. Acad. Sci. USA* **105**, 329–334 (2008).
34. Viskontas, I.V., Knowlton, B.J., Steinmetz, P.N. & Fried, I. Differences in mnemonic processing by neurons in the human hippocampus and parahippocampal regions. *J. Cogn. Neurosci.* **18**, 1654–1662 (2006).
35. Axmacher, N. *et al.* Intracranial EEG correlates of expectancy and memory formation in the human hippocampus and nucleus accumbens. *Neuron* **65**, 541–549 (2010).
36. Köhler, S., Danckert, S., Gati, J.S. & Menon, R.S. Novelty responses to relational and non relational information in the hippocampus and the parahippocampal region: A comparison based on event related fMRI. *Hippocampus* **15**, 763–774 (2005).
37. Kumaran, D. & Maguire, E.A. Novelty signals: a window into hippocampal information processing. *Trends Cogn. Sci.* **13**, 47–54 (2009).
38. Grunwald, T. *et al.* Dissecting out conscious and unconscious memory (sub)processes within the human medial temporal lobe. *Neuroimage* **20** (suppl. 1), S139–S145 (2003).
39. Meunier, M., Bachevalier, J., Mishkin, M. & Murray, E.A. Effects on visual recognition of combined and separate ablations of the entorhinal and PrC in rhesus monkeys. *J. Neurosci.* **13**, 5418–5432 (1993).
40. Murray, E.A. & Richmond, B.J. Role of PrC in object perception, memory, and associations. *Curr. Opin. Neurobiol.* **11**, 188–193 (2001).
41. Gonsalves, B.D., Kahn, I., Curran, T., Norman, K.A. & Wagner, A.D. Memory strength and repetition suppression: multimodal imaging of medial temporal cortical contributions to recognition. *Neuron* **47**, 751–761 (2005).
42. Henson, R.N., Cansino, S., Herron, J., Robb, W. & Rugg, M. A familiarity signal in human anterior medial temporal cortex? *Hippocampus* **13**, 301–304 (2003).
43. Montaldi, D., Spencer, T.J., Roberts, N. & Mayes, A.R. The neural system that mediates familiarity memory. *Hippocampus* **16**, 504–520 (2006).
44. Grunwald, T., Lehnertz, K., Heinze, H.J., Helmstaedter, C. & Elger, C.E. Verbal novelty detection within the human hippocampus proper. *Proc. Natl. Acad. Sci. USA* **95**, 3193–3197 (1998).
45. Buckley, M.J. & Gaffan, D. Perirhinal cortex ablation impairs configural learning and paired-associate learning equally. *Neuropsychologia* **36**, 535–546 (1998).
46. Higuchi, S. & Miyashita, Y. Formation of mnemonic neuronal responses to visual paired associates in inferotemporal cortex is impaired by perirhinal and entorhinal lesions. *Proc. Natl. Acad. Sci. USA* **93**, 739–743 (1996).
47. Staresina, B.P. & Davachi, L. Differential encoding mechanisms for subsequent associative recognition and free recall. *J. Neurosci.* **26**, 9162–9172 (2006).
48. Diana, R.A., Yonelinas, A.P. & Ranganath, C. Medial temporal lobe activity during source retrieval reflects information type, not memory strength. *J. Cogn. Neurosci.* **22**, 1808–1818 (2010).
49. Takeuchi, D., Hirabayashi, T., Tamura, K. & Miyashita, Y. Reversal of interlaminar signal between sensory and memory processing in monkey temporal cortex. *Science* **331**, 1443–1447 (2011).
50. Gelbard-Sagiv, H., Mukamel, R., Harel, M., Malach, R. & Fried, I. Internally generated reactivation of single neurons in human hippocampus during free recall. *Science* **322**, 96–101 (2008).

ONLINE METHODS

fMRI study. Twenty (14 female) right-handed native English speakers with normal or corrected-to-normal vision participated in the experiment (mean age = 28 years, range = 20–35). Informed consent was obtained in a manner approved by the Cambridge Psychological Research Ethics Committee and participants were paid for their participation.

The stimulus material consisted of 360 English nouns and eight different associated source details: the colors blue, green, red and yellow, and the scenes office, living room, city and nature. Each study or test block used only one category (colors or scenes), and color and scene blocks were alternated, with the assignment of the first block counterbalanced across participants. As all experimental parameters were identical for color and scene runs, and because we observed no performance differences (**Supplementary Results**), data from color and scene blocks were collapsed for the current analysis to increase statistical power. The assignment of nouns to the list of study items or lures for the test phase and to color versus scene blocks was randomized across participants.

During each study block, participants saw 60 nouns together with one of four possible sources. Nouns were presented in white uppercase letters and centered on a black background. The associated source (a color or scene, depending on the current block) was presented in a 250 × 350 pixels frame positioned 150 pixels underneath the noun. A given noun/source combination was presented on the screen for 4 s and participants indicated whether the given combination was plausible or implausible[47]. Participants were encouraged to give their response as fast as possible. All four study blocks were presented in a row (with a short break in between), followed by a 5-min break, during which the anatomical scan was acquired, and then all four test blocks were presented in a row (again with a short break in between). A test block contained all 60 previously seen (studied) nouns as well as 30 experimentally novel (unstudied) nouns (lures). The lures were pseudorandomly intermixed, holding the average delay between study and test constant across nouns. Upon being presented with a noun, participants could give one of six possible answers: (i) new (item not seen during the study phase), (ii) old, seen with source 1 (blue or office for color and scene runs, respectively), (iii) old, seen with source 2 (green or living room for color and scene runs, respectively), (iv) old, seen with source 3 (red or city for color and scene runs, respectively), (v) old, seen with source 4 (yellow or nature for color and scene runs, respectively), or (vi) old, but cannot remember the source ("don't know" response). Thus, participants indicated with one button press whether they thought the noun was old or new and whether they also remembered the studied source detail. Both study and test trials were presented at a fixed duration of 4 s. Trials were pseudorandomly intermixed with an active arrows task to maximize the efficiency of the rapid event-related design (see below).

The experimental procedure yielded three conditions of interest: unstudied items correctly identified as new (correct rejection), studied items correctly identified as old, without remembering the correct source from the study episode (item recognition), and studied items correctly identified as old, also remembering the correct source (source recognition). For item recognition, to increase statistical power, we collapsed trials for which participants gave "don't know" responses and trials for which the wrong source was indicated. However, results remained unchanged when including only "don't know" responses (with the exception that one iEEG participant had to be excluded for providing an insufficient number of trials). Misses (studied items incorrectly classified as new) and false alarms (unstudied items incorrectly classified as old) were not included in the analysis. On average, there were 97 correct rejection trials (range, 39–118), 88 item recognition trials (range, 38–140) and 118 source recognition trials (range, 34–186) across the fMRI participants.

Scanning was performed on a 3-T Siemens Tim Trio MRI system using a 32-channel whole-head coil. Functional data were acquired using a gradient-echo, echo-planar pulse sequence (repetition time = 2,000 ms, echo time = 30 ms, 32 horizontal slices oriented parallel to the hippocampal axis, descending slice acquisition, 3 × 3 × 3 mm voxel size, 0.75-mm inter-slice gap, 165 and 245 volume acquisitions per study and test session, respectively). The first seven volumes of each session were discarded to allow for magnetic field stabilization. High-resolution (1 × 1 × 1 mm) T1-weighted (MP-RAGE) images were collected for anatomical visualization. Foam padding was used to minimize head motion. Visual stimuli were projected onto a screen that was viewed through a mirror and responses were collected with magnet-compatible button boxes placed under the participant's hands. Stimuli were created and presented using the Psychophysics Toolbox[51] implemented in MATLAB.

Both the study and the test portion of the experiment were scanned, but only test data are reported here. Trials were intermixed with an active, sensorimotor baseline task (arrows task[52], comprising a fourth of the total scanning time). Arrows that randomly pointed to the left or to the right for 1 s were repeatedly presented for the length of a baseline trial (2–10 s), and participants had to press the left hand index finger key if the arrow pointed to the left and the right hand index finger key if it pointed to the right. The sequence of old trials associated with each of the four possible sources, new trials and the variable number of baseline trials, was pseudorandom and optimized for rapid event-related fMRI (using the optseq algorithm[53]).

Data were analyzed using SPM8 (http://www.fil.ion.ucl.ac.uk/spm/). During preprocessing, images were corrected for differences in slice acquisition timing, followed by motion correction across all sessions. We analyzed retrieval-related BOLD responses in hippocampus and PrC using hand-drawn, participant-specific ROIs on the basis of the individual structural image (for whole-brain results, see **Supplementary Table 2**). Note that no smoothing was performed on the data, ensuring that there was minimal signal overlap between the hippocampus and the adjacent PrC. Anatomical demarcation was carried out as described previously[54]. Because the iEEG data were obtained from the anterior hippocampus, the anterior part of the hippocampus used for the fMRI data was defined as the anterior half of its full longitudinal extent. Given that the iEEG data were recorded from both left and right hemispheres across participants, we collapsed left and right perirhinal and hippocampal ROIs, respectively, for the ROI analysis. In both resulting ROIs (hippocampus, PrC), we extracted the percent signal change for each condition of interest via the MarsBaR toolbox[55]. To extract the peristimulus BOLD signal change, we fit a finite impulse response (FIR) basis set, with bin-width equal to the TR, to each condition in a design matrix that concatenated all test blocks and modeled head movement, low-frequency scanner drift and run means as nuisance regressors. BOLD time series were extracted from trial onset (TR0) to TR5 post stimulus onset. Given that data were aligned to the middle slice during preprocessing, this sampling effectively covered 1–11 s post stimulus onset. Analogous to baseline correction in the EEG data, the first TR was subtracted from each condition to align the starting point of the BOLD time series across conditions. Consequently, only TRs 1–4 (3–9 s post stimulus onset) entered statistical analyses of BOLD data. Note, however, that the same pattern of results emerged when not baseline correcting. For the analyses of BOLD time courses, the FIR parameter estimates were averaged across voxels in each ROI in the participant's native space, and the resulting values were used in group-level ANOVAs and t tests.

The more conventional analysis of our fMRI data was based on the same conditions and onsets, but used a single, canonical HRF, as provided in SPM8, instead of the above FIR basis set. The neural activity was modeled as an epoch (boxcar) with a duration equal to the trial-specific response time, although the same pattern of results was obtained when modeling each trial as an impulse (delta function) or as a fixed-length 4-s epoch.

Functional connectivity was examined in the SPM8 toolbox for PPIs. Given our a priori predictions for hippocampal-perirhinal coupling, we used the bilateral hippocampus ROIs as the seed region and corrected results via small-volume correction (SVC) where all individual bilateral perirhinal masks were normalized and combined, resulting in a 18,872-mm^3 mask used for SVC. The PPI analysis was designed to identify voxels in which functional connectivity with the hippocampal seed was greater for source recognition than for item recognition trials. When thresholding the results at $P < 0.001$ uncorrected, one cluster appeared in left PrC and one appeared in right PrC, which survived correction at the set level (that is, probability of $P < 0.05$ of two such clusters within the bilateral perirhinal mask image).

iEEG study. iEEG was recorded from patients suffering from pharmaco-resistant epilepsy. Depth electrodes comprising ten platinum contacts were implanted stereotactically along the longitudinal axis of each MTL (**Fig. 1b**) during presurgical evaluation. Depth electroencephalograms were referenced to linked mastoids and recorded with a sampling rate of 1 kHz. A total of eight patients with the same MTL implantation scheme participated in the study, of which three patients did not meet all inclusion criteria (detailed below). In four of the five patients included in the analysis (three female), iEEG recordings identified a unilateral seizure onset zone in the MTL, and only data from the contralateral hemisphere were used for analyses. For the remaining male patient, no seizure onset zone was identified in the MTL of either hemisphere and data from the left hemisphere were used according to the selection criteria described below. Thus, right hemisphere data

were used from three patients and left hemisphere data from the remaining two patients. Patients ranged in age from 19 to 51 years (mean 34 years) and in duration of their epilepsy from 8 to 46 years (mean 22 years). At the time of the recordings, all patients received anticonvulsive medication (plasma levels in the therapeutic range). Informed consent for the iEEG recordings and the use of the data for research purposes was obtained from all patients. The study was approved by the ethics committee of the Medical Faculty of the University of Bonn.

The experiment was conducted in a sound-attenuated room, with the participant sitting upright in a comfortable chair. A laptop computer, used for stimulus presentation, was positioned on a table at a ~50-cm distance.

The procedure was identical to the fMRI version described above, with the following modifications. First, we decreased task difficulty by decreasing the number of associated sources from four to two (colors: blue, red; scenes: office, nature), decreasing the study list length from 60 items to 50 per block and the test list length from 90 to 75 per block, and conducting six study-delay-test cycles rather than presenting all study blocks and then presenting all test blocks. A study block was followed by a 60-s distraction period during which the participant conversed with the experimenter. These adjustments had the desired effect of improving performance in patients to levels comparable to those of our healthy control group (**Table 1**). One participant did all six cycles in one session, three participants did the first four cycles in one session and the remaining two cycles in another session the same day, and one participant did the first four cycles in one session and the remaining two cycles in another session the next day. One cycle lasted 9 min. Stimuli were presented using Presentation (Neurobehavioral Systems). The whole iEEG experiment lasted ~1 h.

Second, the trial timing was adapted for the iEEG version in the following fashion. In the study phase, participants were given 3 s to make their plausibility judgment. Each trial was preceded by a jittered intertrial interval (700–1,300 ms, mean = 1,000 ms) during which a fixation cross was shown in the center of the screen. In the test phase, responses were given in a self-paced manner, with an upper time limit of 5 s (only three responses were given after 5 s across all participants). Again, each trial was preceded by a jittered intertrial interval (700–1,300 ms, mean = 1,000 ms) showing a fixation cross. Finally, German nouns were used instead of English nouns.

Perirhinal cortex and hippocampus contacts were selected on the basis of anatomical and functional properties. First, only contacts located in PrC and anterior hippocampus were considered. To this end, we co-registered the post-implantation MRI to the pre-implantation MRI, assessing correspondence of individual electrode contacts with anatomical landmarks of PrC and hippocampus[54] (**Fig. 1b**). In three of the five patients, the selected contact was clearly located in PrC, whereas the contact was located between peri- and entorhinal cortex for the remaining two patients. However, there was no qualitative difference in the overall response profiles and we refer to the ento- and perirhinal contact as perirhinal for brevity. Given the prototypical negative component (N400) characterizing functional ento-/perirhinal recordings[56,57], we further required the PrC response profile to contain a clear negative peak in the first second post stimulus onset. A peak was defined as any time point whose negative amplitude exceeded two s.d. of all negative values from 0–2 s, based on the average of all conditions of interest (correct rejection, item recognition, source recognition) to avoid any selection bias. The three participants who were excluded failed to show a negative peak. If more than one contact fulfilled the criteria for PrC and hippocampus selection, we chose the contact with the highest absolute amplitude (baseline corrected) summed across the first second. **Supplementary Table 1** lists the approximate MNI coordinates of the selected PrC and hippocampus contacts after segmentation and normalization to a T1-weighted MRI template via SPM8.

Finally, we performed additional analyses to ensure that activation in the selected perirhinal and hippocampal contacts does not reflect a single common ERP generator/signal source. First, we plotted the raw signal of all contacts along each participant's depth electrode, confirming different peak latencies along with pronounced spatial gradients along the anterior-posterior implantation axis between the selected perirhinal and hippocampal contacts. Second, we used spectral coherence analyses across pairwise combinations of adjacent contacts to identify functional transitions (as reflected in a drop of coherence) across contact pairs. The results of these analyses (**Supplementary Results** and **Supplementary Fig. 2**) confirmed the functional-anatomical boundary between our PrC and hippocampal contacts.

Artifact rejection was performed on trial epochs from −1 to 3 s time locked to stimulus onset. Prior to manual artifact rejection, an automated procedure was implemented in MATLAB to reject trials in which at least one time point in PrC or hippocampus exceeded three interquartile ranges of all trial-specific values in both amplitude and gradient (difference to previous time point). Across participants, an average of 26% (range, 16–39%) of all trials from the recognition memory phase were excluded. On average, there were 87 correct rejection trials (range, 32–115), 104 item recognition trials (range, 50–155) and 85 source recognition trials (range, 34–162) across participants after artifact rejection.

Statistical analyses were performed on the unfiltered raw ERPs after baseline correction (subtracting the average 100-ms prestimulus interval), using repeated-measures ANOVAs (with a Greenhouse-Geisser correction for correlated errors) and pairwise, two-tailed t tests. Response-triggered averages (**Fig. 3**) were computed by cutting out a 2-s time window centered on each trial's reaction time, and only data points after stimulus onset were included in the averages. To compare item and source effects directly across pre- versus post-response time windows, we defined the effects as the numerically larger condition minus the numerically smaller condition across participants, so that the sign of the average effects was the same. For identifying the effect onset latencies (**Fig. 4**), we computed a sliding average across a 100-ms time window that moved forward in 50-ms increments and subjected the resulting values to paired t tests across conditions of interest.

Time-resolved spectral coherence between hippocampus and PrC was calculated using the FieldTrip toolbox[58]. Because the coherence measure is biased by the number of trials, we equated the trial numbers across conditions by subselecting a random portion of the condition with more trials to match the condition with fewer trials. This was repeated ten times and the resulting coherence values of the ten subsamples from the condition with more trials were averaged in each participant. Frequency decomposition was achieved via Fourier analysis based on sliding time windows (moving forward in 10-ms increments). The settings were optimized for two frequency ranges. For a lower frequency range (1–29 Hz, 1-Hz steps), the window length was set to four cycles of a given frequency (for example, 400 ms for 10 Hz; 200 ms for 20 Hz), and the windowed data segments were multiplied with a Hanning taper before Fourier analysis. For higher frequencies (30–100 Hz, 5-Hz steps), we applied multitapering, using a fixed window length of 200 ms and three orthogonal Slepian tapers (resulting in spectral smoothing of ~10Hz) (this approach was adopted from refs. 59,60). The resulting coherence maps were baseline corrected (subtracting a −400 to −200-ms time interval) and subjected to direct comparison between source recognition and item recognition. We focused our analyses on two frequency bands: low gamma (30–50 Hz), where increased coupling between hippocampus and rhinal cortex during successful memory encoding has been reported[24], and on lower frequencies from 1 to 29 Hz. Because we did not have a priori hypotheses about the exact frequencies or the time intervals at which to expect differences, we corrected for multiple comparisons across frequencies (1–29 Hz and 30–50 Hz) and time points (0–2 s) using a cluster-based permutation approach[23] (alpha = 0.05). It should be noted that no additional effect emerged when we extended the gamma range to 100 Hz. The same procedure was repeated to compare hippocampal-perirhinal coherence for correct rejection versus item recognition.

51. Brainard, D.H. The Psychophysics Toolbox. *Spat. Vis.* **10**, 433–436 (1997).
52. Stark, C.E. & Squire, L.R. When zero is not zero: the problem of ambiguous baseline conditions in fMRI. *Proc. Natl. Acad. Sci. USA* **98**, 12760–12766 (2001).
53. Dale, A.M. Optimal experimental design for event-related fMRI. *Hum. Brain Mapp.* **8**, 109–114 (1999).
54. Insausti, R. *et al.* MR volumetric analysis of the human entorhinal, perirhinal, and temporopolar cortices. *AJNR Am. J. Neuroradiol.* **19**, 659–671 (1998).
55. Brett, M., Anton, J.-L., Valabregue, R. & Poline, J.-B. Region of interest analysis using an SPM toolbox [abstract]. in *8th Int. Conf. Funct. Mapp. Hum. Brain* (eds. R. Kawashima, H. Sakata, K. Nakamura & M. Taira) **497** (Academic Press, 2002).
56. McCarthy, G., Nobre, A.C., Bentin, S. & Spencer, D.D. Language-related field potentials in the anterior-medial temporal lobe. I. Intracranial distribution and neural generators. *J. Neurosci.* **15**, 1080–1089 (1995).
57. Smith, M.E., Stapleton, J.M. & Halgren, E. Human medial temporal lobe potentials evoked in memory and language tasks. *Electroencephalogr. Clin. Neurophysiol.* **63**, 145–159 (1986).
58. Oostenveld, R., Fries, P., Maris, E. & Schoffelen, J.M. FieldTrip: open source software for advanced analysis of MEG, EEG, and invasive electrophysiological data. *Comput. Intell. Neurosci.* **2011**, 156869 (2011).
59. Jokisch, D. & Jensen, O. Modulation of gamma and alpha activity during a working memory task engaging the dorsal or ventral stream. *J. Neurosci.* **27**, 3244–3251 (2007).
60. Meeuwissen, E.B., Takashima, A., Fernández, G. & Jensen, O. Increase in posterior alpha activity during rehearsal predicts successful long-term memory formation of word sequences. *Hum. Brain Mapp.* **32**, 2045–2053 (2011).